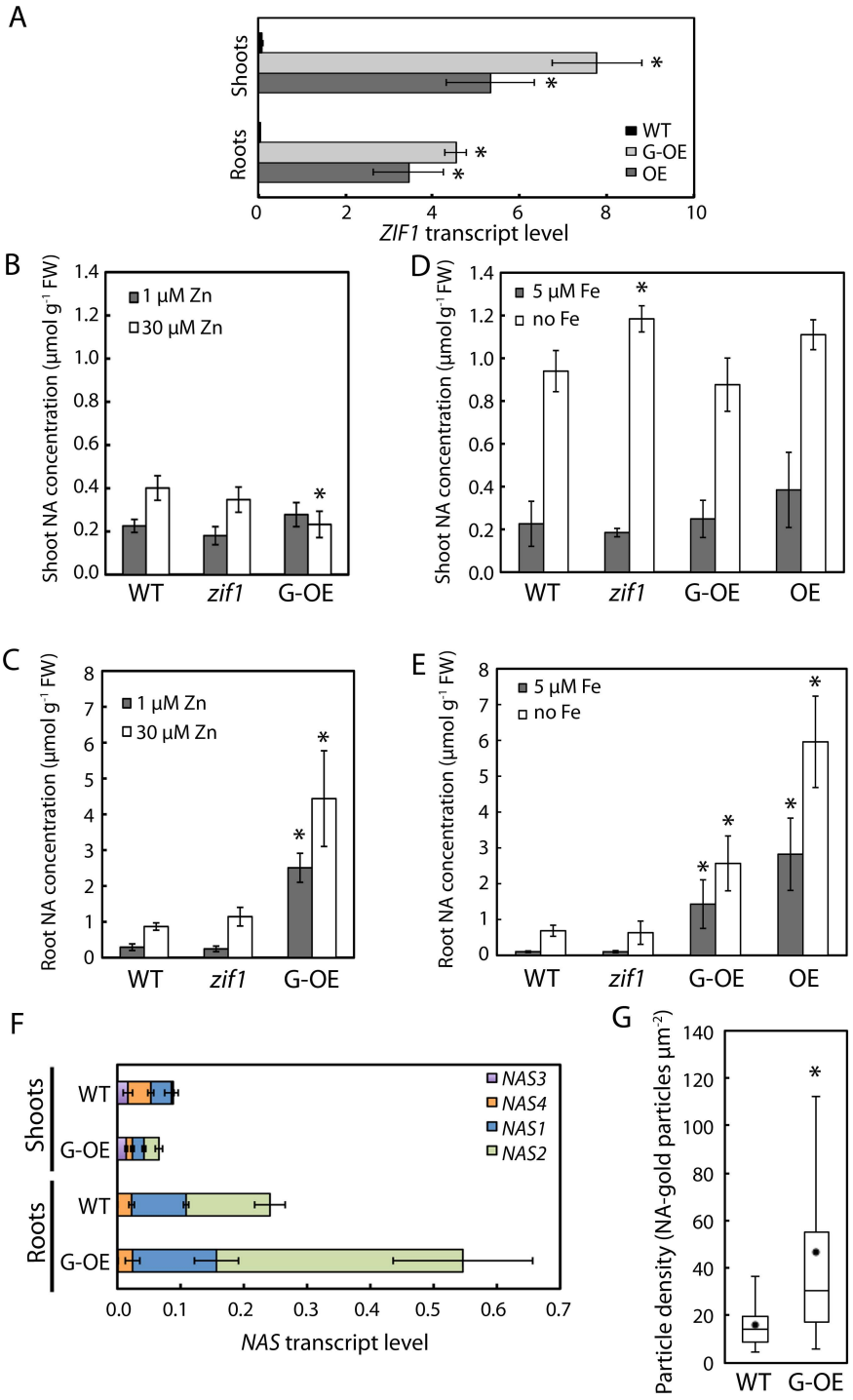

Supplemental Figure 1. Effect of *ZIF1* overexpression on NA concentrations and *NAS* transcript levels.
(A) Transcript levels of *ZIF1*, relative to *UBQ10* and *ACT2*, in Col (WT) and 35S-*ZIF1-GFP* (G-OE) and 35S-*ZIF1* (G-OE) grown on control media, determined by qRT-PCR (mean ± SD, *n* =3).
(B) Shoot and **(C)** root NA concentrations in 23-d-old Col, *zif1*-3 and 35S-*ZIF1-GFP* seedlings grown on control media or supplemented with 30 µM Zn for 16 d (mean ± SD, *n* = 6).
(D) Shoot and **(E)** root NA concentrations of 20-d-old Col, *zif1*-3, 35S-*ZIF1-GFP* and 35S-*ZIF1* seedlings grown on control or Fe-deficient (no Fe) media for 10 d (mean ± SD, *n* = 4).
Asterisks in **(A), (B), (C), (D)** and **(E)** denote significant difference from WT by Student's *t*-test, with Bonferroni corrections ($P < 0.05$).
(F) Transcript levels of *NAS1, NAS2, NAS3* and *NAS4*, relative to *UBQ10*, in shoots and roots of 21-d-old Col and 35S-*ZIF1-GFP* seedlings grown on control media, determined by qRT-PCR (mean ± SD, *n* = 3).
(G) Quantification of total immunogold-labelled NA in TEM images of Col and 35S-*ZIF1-GFP* root tips. Gold particles were counted and normalized to area in 19 images per genotype. Values are median (line), lower and upper quartiles (boxes); error bars represent minima and maxima; black dots indicate means. Asterisk denotes significant difference from WT by Mann-Whitney test ($P < 0.001$).

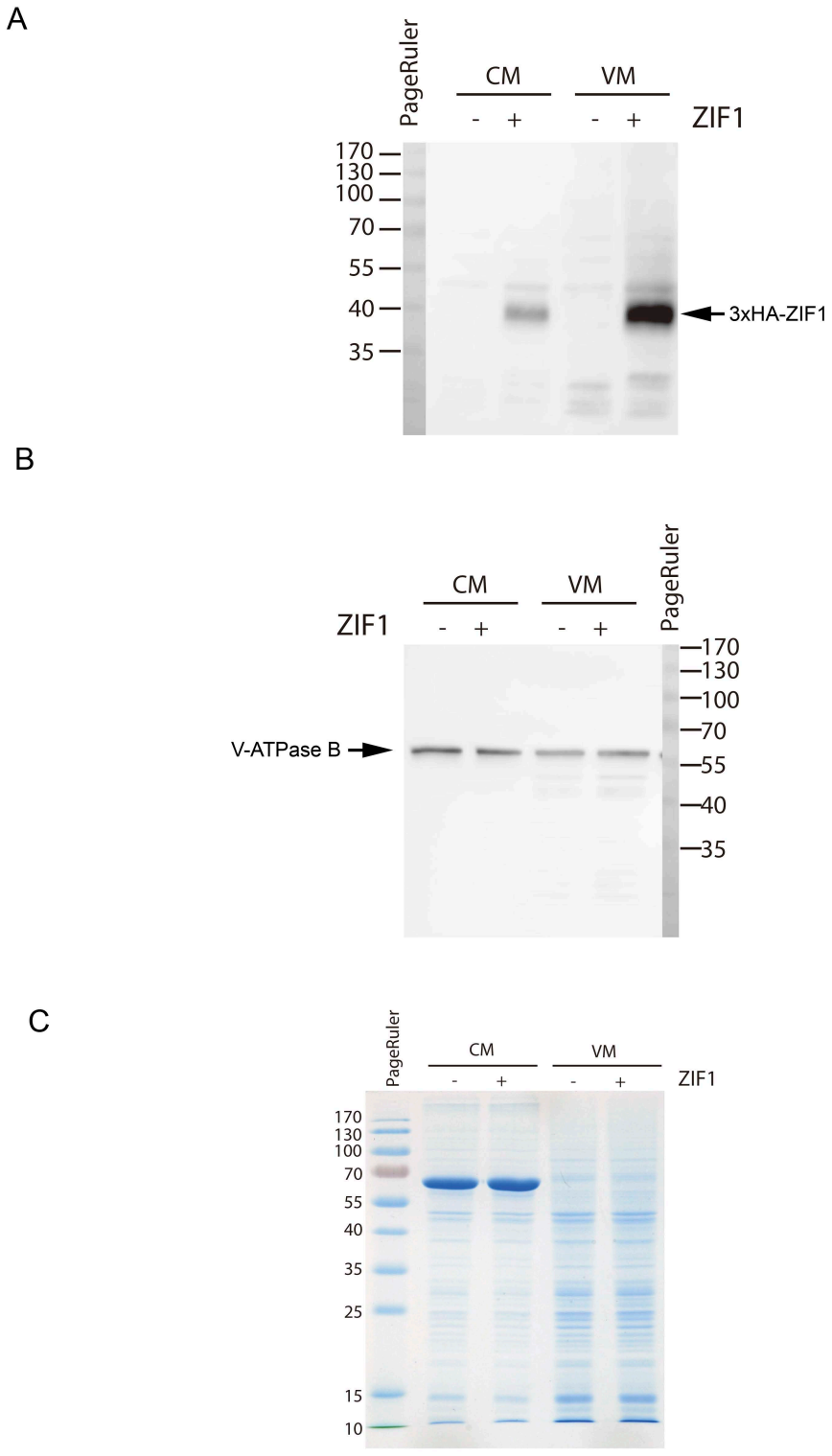

Supplemental Figure 2. Detection of 3xHA-ZIF1 in the vacuolar membrane of yeast.
Immunoblots of total crude membrane (CM) and vacuole-enriched membrane (VM) preparations from wild-type yeast (BY4741) transformed with ZIF1-pFL383 (+ ZIF1) or pFL38 (- ZIF1). 5 mg protein per lane was separated on 12% SDS-PAGE gels. Approximate sizes in kDa of the protein marker are given.
(A) Detection of 3xHA-ZIF1 with anti-HA in yeast memrane fractions.
(B) Detection of vacuolar ATPase subunit B with anti-V-ATPase in yeast membrane fractions
(C) Coomassie blue stained gel of protein samples shown in **(A)** and **(B)**.

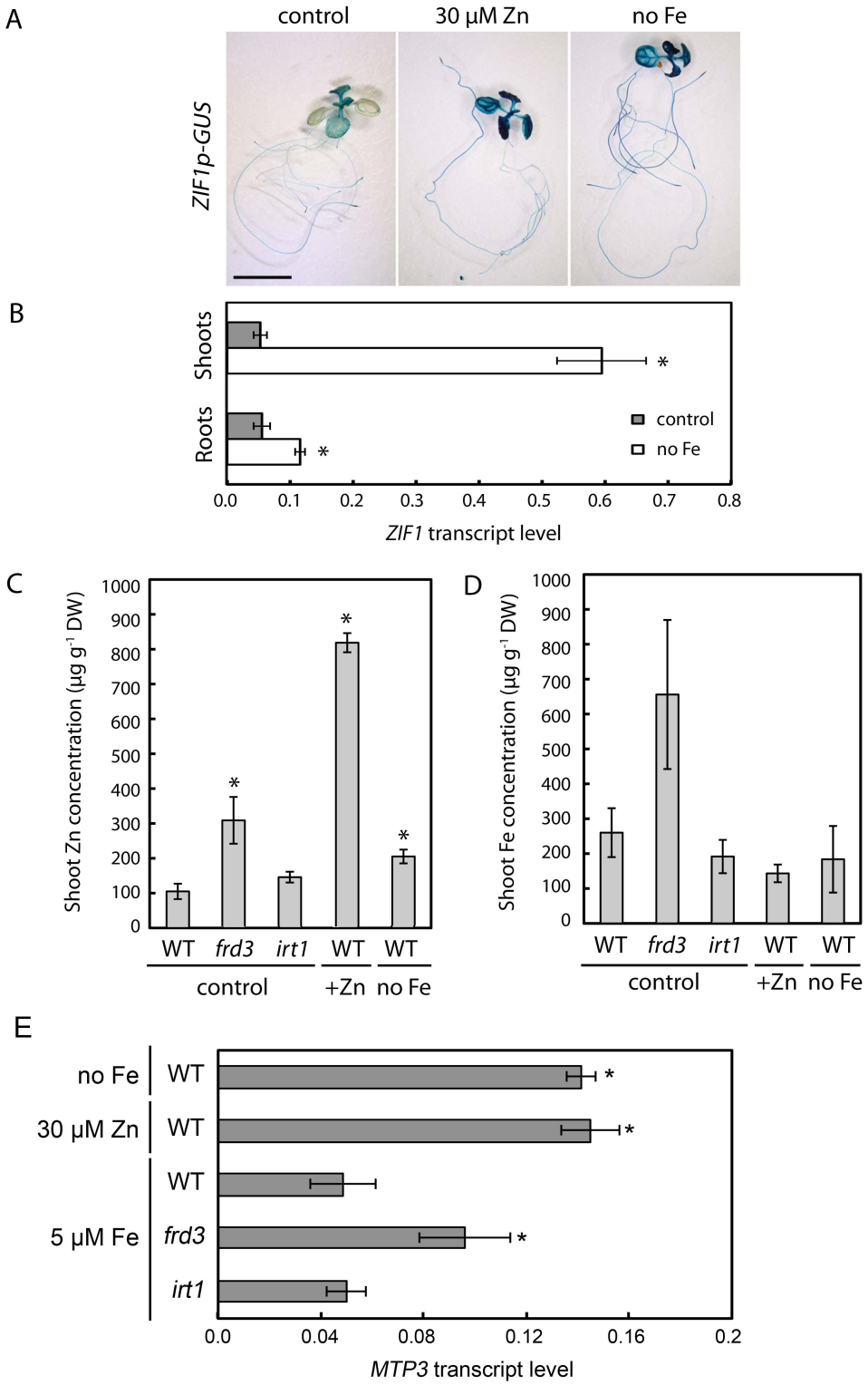

Supplemental Figure 3. Fe-dependent regulation of *ZIF1* promoter activity and transcript levels.
(A) *ZIF1* promoter activity in seedlings grown on control, high Zn (30 µM Zn) or Fe deficient (no Fe) media for 7 d. Images are of 14-d-old *ZIF1prom-GUS* transgenic seedlings following histochemical staining for β-glucuronidase activity. Bar: 10 mm.
(B) Transcript levels of *ZIF1*, relative to *UBQ10* and *ACT2*, in shoots and roots of 14-d-old Col (WT) seedlings grown on control or Fe-deficient (no Fe) media for 3 d, determined by qRT-PCR (mean ± SD, $n = 3$).
(C) Shoot Zn and **(D)** Fe concentrations in 17-d-old Col (WT), *frd3*-1 and *pam25* (*irt1*) seedlings grown on control media compared to WT seedlings grown on Fe deficient (no Fe) or high Zn (30 µM Zn) media for 7 d, determined by ICP-AES (mean ± SD, $n = 4$).
(E) Transcript levels of *MTP3*, relative to *UBQ10*, in roots of 17-d-old Col (WT), *frd3*-1 and *pam25* (*irt1*) seedlings grown on control media and WT grown on Fe-deficient (no Fe) or Zn-supplemented (30 µM) media for 7 d, determined by qRT-PCR (mean ± SD, $n = 3$).
Asterisks in **(B), (C), (D)** and **(E)** denote significant differences from WT by Student's *t*-test with Bonferroni corrections ($P < 0.05$).

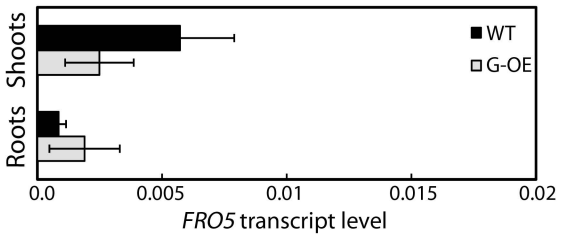

Supplemental Figure 4. *ZIF1* overexpressors do not upregulate *FRO5*, a transcriptional marker of Cu-deficiency. Transcript levels the Cu-deficiency marker, *FRO5*, relative to *UBQ10*, in shoots and roots of 21-d-old Col and 35S-*ZIF1-GFP* seedlings grown on control media, determined by qRT-PCR (mean ± SD, $n = 3$). No significant differences from WT were detected by Student's *t*-test, with Bonferroni corrections ($P < 0.05$).

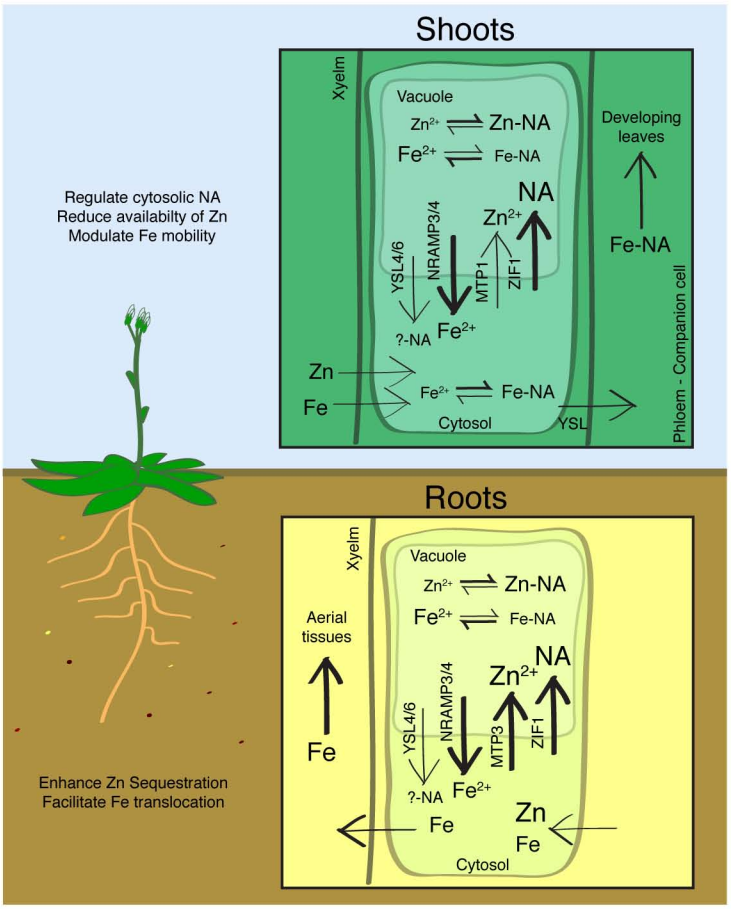

Supplemental Figure 5. Proposed working model for ZIF1 function under micronutrient stress.

In plants exposed to excess Zn or low Fe, influx of Zn into the cytoplasm of root cells is enhanced. Under these conditions, *ZIF1* expression levels are strongly upregulated, and expression domains expand beyond the vasculature in both roots and shoots. Thus, expression levels and patterns of *ZIF1* in 35S-*ZIF1* transgenic lines resemble those found naturally under Fe deficiency and excess Zn.

Once Zn has entered root epidermal and cortex cells of plants cultivated under Fe deficiency or excess Zn conditions, Zn^{2+} is transported into vacuoles by MTP3. Cytoplasmic NA synthesis is upregulated. The transport of NA into the vacuole is proposed here to involve ZIF1. At vacuolar pH, equilibrium favours the formation of Zn-NA over free Zn^{2+}. It is not known how Fe is transported into the vacuoles of these cells, but inside the vacuole, the presence of free Fe^{2+} is predicted to be favoured over Fe^{II}-NA.

Thus, high vacuolar NA concentrations promote the vacuolar sequestration of Zn, thus limiting the flux of Zn towards the xylem and into shoots. Iron concentrations in *ZIF1* overexpressing lines additionally suggest that the sequestration of NA and Zn in the vacuole of root cells acts to enhance the mobility of Fe for root-to-shoot translocation, whereas it acts to decrease the mobility of Zn for root-to-shoot transport in the xylem. Therefore, enhanced *ZIF1* expression helps plants to maintain their micronutrient balance under conditions of enhanced Zn influx into roots as experienced in Fe-deficient and excess-Zn growth conditions.

NRAMP3 and NRAMP4, which are known to be present in the root vasculature and increase in abundance under Fe deficiency, mobilize free Fe^{2+} from vacuoles. NRAMP4 can also transport Zn^{2+}. YSL4 and YSL6, which localize to the vacuolar membrane, are proposed to mobilize undefined metal-NA complexes from the vacuole.

In shoots, increased accumulation of NA inside vacuoles involving ZIF1 enhances the sequestration potential for Zn in vacuoles, as in roots. At cytosolic pH, in contrast to inside vacuoles, equilibrium favours formation of Fe-NA complexes. By limiting the cytosolic concentration of NA through its sequestration in the vacuole, ZIF1 might increase availability of free Fe for local cellular processes. Conversely, Fe-NA complexes would serve as substrate for Fe-NA transporters. It is not known how Fe is exported from leaf cells but uptake of Fe-NA into phloem companion cells by YSL transporters facilitates the transport of Fe to developing tissues, and the transported form of Fe in the phloem was proposed to be Fe-NA. Thus, ZIF1 may act to restrict cytoplasmic NA availability and, as a consequence, the export of Fe from source leaves *via* the phloem in order to conserve photosynthesis functions. This is consistent with interveinal chlorosis predominating in young leaves of both *ZIF1* overexpressors and mutants impaired in NA biosynthesis. As it would be harmful to excessively starve young leaves of iron, this might also explain the need to restrict the extent to which *ZIF1* expression is upregulated under iron deficient growth conditions through the repressive action of the bHLH transcription factor POPEYE.

It should be noted that the increased influx of Zn into plants grown under conditions of Fe deficiency or excess Zn, in which *ZIF1* expression is naturally upregulated, would preclude the occurrence of Zn deficiency, contrary to the situation in *ZIF1* overexpressors.

In summary, through balanced regulation of ZIF1-dependent NA compartmentalization between the cytosol and the vacuole, ZIF1 might facilitate the mobilization of Fe from the vacuole while enhancing sequestration of Zn, increase the local availability of Fe^{2+} in the cytosol, and modulate the transport of Fe-NA complexes to developing tissues *via* the phloem. Overall, based on our results and previous work on NA-deficient mutants, ZIF1 and cytoplasmic NA availability appear to primarily affect the xylem transport pathway for Zn, but not for Fe. By contrast, for Fe, the primary transport pathway affected is through the phloem which is also affected for Zn.

Thick and thin arrows indicate strong or weak flux, respectively. Font size of metal ions and metal complexes indicate relative concentrations within various cellular and subcellular compartments.

Supplemental Table 1. Sequences of primers used for quantitative real-time PCR

Gene	Forward (5'-3')	Reverse (5'-3')
UBQ10	GGCCTTGTATAATCCCTGATGAATAAG	AAAGAGATAACAGGAACGGAAACATAGT
EF1α	TGAGCACGCTCTTCTTGCTTTCA	GGTGGTGGCATCCATCTTGTTACA
ZIF1	CAGGCTTGTCAGGTCTCAGTC	GCTACTCCGACCACTACTATCAC
NAS1	CATGATCTTCCACACAACGGAC	CGACGTCATATTGGTCAAGGC
NAS2	CTGACGACGTGGTTAATTCGG	TGCCTCGAGCTCCATTTGA
NAS3	ACGAACAATTGGTGCAAACA	GAGAATGTTGACATCTTCGG
NAS4	ACGACCAACTCGTAAACAAG	GAGAGTGTCGACATCTTCAC
ZIP4	AGCAAGAGAGGAATCAGGCTGC	CCAACCACAGGAACAACAGCA
ZIP9	CCATCACTACTCCGATCGGTGT	CACCAATGCTGCAACGCTATAA
IRT1	CCCCGCAAATGATGTTACCTT	GGTATCGCAAGAGCTGTGCAT
MTP3	TTTGCCTTCCATCCCGAA	CTGATGTTGCAGCCTTTGCA
FRO3	AAACGTTGACGCATTGTCTCC	GGTGAATTCCGGTAGCAACTG
FRO5	TACCCAAAAGCAACCCTCCC	ATCATCACCCTCCCCATTCT